TELKOMNIKA, Vol. 11, No. 7, July 2013, pp. 3684 ~ 3692
e-ISSN: 2087-278X

A Novel Design of Aircraft Fuel Tank Inspection Robot

Guochen Niu*, Zunchao Zheng, Qingji Gao , Weijuan Wang, Lei Wang
Robotics Institute, Civil Aviation University of China, Telp/Fax: 022-24092609
JinBei Road No. 2898, Tianjin 300300, China
Corresponding author, e-mail: niu_guochen@139.com

Abstract

Aircraft fuel tank leakage is a very common maintenance problem. A continuum robot is designed for troubleshooting of leaks for fuel tank which has strong constraints and is also explosive. The biomimetic robot with several flexible sections applies actuation redundancy through pulling its four independent driving cables to realize bending motion of two degrees of freedom (DOF). The forward kinematics about the relations of cables lengths, angles and tip coordinates of single section is established using projection curvature method and coordinates transformation method. The decoupled multi-section kinematics function is deduced based on the kinematics analysis of single section. Simulations of single section motion are presented. We demonstrate finally the correctness of kinematics method through prototype experiments.

Keywords*: aircraft fuel tank, continuum robot, kinematics, leak inspection*

1. Introduction

Internal environment of aircraft fuel tank is complicated and narrow since uniform stringers, fuel pipes and related facilities distribute in the aircraft fuel tank. Meanwhile, the fuel tank is full of many kinds of toxic gases, so it is difficult for aircrews to operate in fuel tank. Nowadays, leak and corrosion inspection of fuel tank is mainly dependent on Crewe to operate in aircraft fuel tank, so a semi-automatic device is in urgently need to improve maintenance efficiency and reduce labor intensity. Continuum robot which has such biological features as snakes, elephant trunks and octopus arms can change its shape to adapt to the environment with strong space constraints like aircraft fuel tank.

In recent years, continuum robot has been extensively studied. In 1999, Robinson et al. [1] firstly proposed the concept of continuum robot. Walker et al. [2-5] developed continuum robot OctArm, using pneumatic artificial muscles as a driver, and each section has two DOF. Simaan et al. [6-8] presented a new kind of continuum robot for throat surgery, which has two bending sections that use elastic NiTi alloy tube equally spaced in the longitudinal direction. Camarillo et al. [9, 10] designed a continuum robot for the examination of human heart disease, which used four-line drive to realize the movement of each segment. Chen et al. [11, 12] developed a continuum robot Clobot installed at the end of the colonoscopy. Webster et al. [13, 14] developed a continuous concentric tube robot composed by the three-band super-elastic NiTi alloy tube. Hu HY et al. [15] proposed a kind of continuum robot for intestinal endoscope using the cable-driven method. However, continuum robots used in aircraft fuel tank inspection is rarely reported.

A snake-like robot with continuous structure for aircraft fuel tank leak detection is designed in this paper. In the following parts, not only the kinematics of continuous single section is deduced, but also decoupled kinematics equation of multi-section is established. Finally, simulation and prototype are proposed to demonstrate the flexible performance and the kinematics method is validated.

2. System Design

The robot is designed for aircraft fuel tank inspection. It adopts a new type of biological structure: continuum structure, a flexible structure characterized by continuously deformable backbone as opposed to the traditional robot featuring rigid links and identifiable rotational

Received January 27, 2013; Revised April 9, 2013; Accepted April 20, 2013

sections. It can bend continuously along its length and produce motion through the generation of smooth curve. In a word, the design needs to fit completely the complicated environmental constraints of aircraft fuel tank.

2.1. Design of Mechanical Structure

Aircraft structure analysis is needed before designing the mechanical structure of robot. As is shown in Figure 1(a), the main tank mainly distributes in the wing and the center tank mianly located in the belly. Figure 1 (b) and (c) depict that internal situation of the wing root position is extremely narrow, and there are many fuel pipes and wires, so wing root position is the most complicated place to enter and detect.

As is shown in Figure 1(d), the designed robot mainly consists of three parts: the Snake Arm, linear module and the moving platform. Flexible Snake Arm enters the interior of the fuel tank for inspecting, rigid linear module in the external of fuel tank supports and positions the Snake Arm, and moving platform provides the support and driving force for other two more modules.

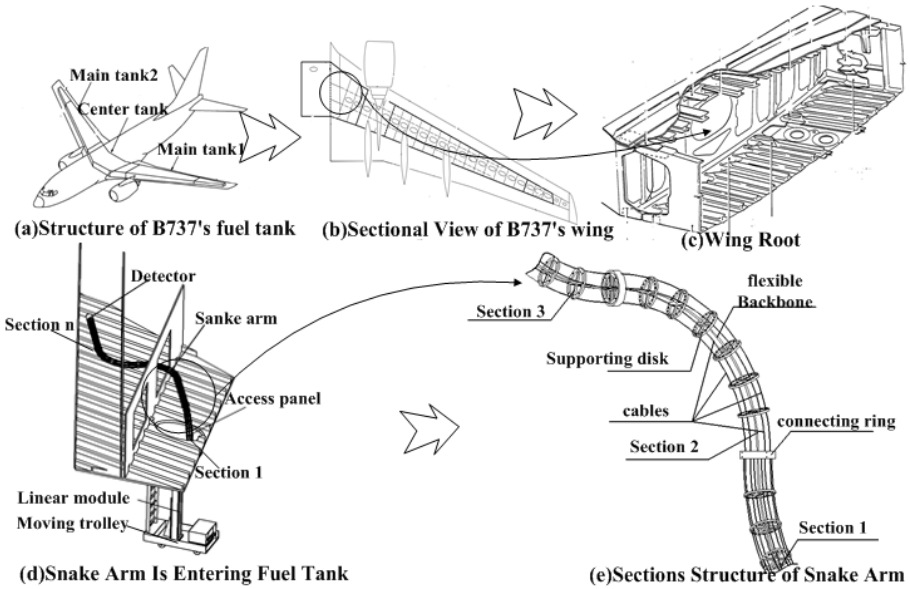

Figure 1. Fuel tank wing root and Snake Arm conformation

Snake Arm has several continuous sections. Each section has two degrees of freedom include bending and rotation motion. Its particular structure is shown in Figure 1(e). Each section consists of some support disks and one flexible backbone. Glass fiber elastic rod as the flexible backbone can support rigidity for the entire sections' shape when Snake Arm bends. Furthermore each section of Snake Arm can bend and rotate through length variation of four driving cables which are uniformly distributed around backbone at intervals of 90°.The cable-driven method makes the control-motors and many electric circuits stay out of fuel tank to radically solve the explosion problems, while reducing weight and inertia of the section in order to make the sections more flexible. Moreover, Snake Arm wrapped with plastic pipes outside can reduce friction between sections and components of fuel tank, and protect the sections from corrosion in the fuel gas environment.

2.2. Design of Control System

The control system of tank inspection robot is mainly composed of three parts: human-machine interface, console and executing unit, as is shown in Figure 2.

1) Human-machine interface: Human-machine interface is developed on the Windows platform using VC++. The main features include: target point setting, image acquisition, path planning and motion control. Firstly, input the coordinates of target point, then the system will

update the real-time coordinates as the input value of path planning module. Secondly, the planning datas are stored in a data file, then the path parameters are loaded and converted by motion control unit to motor motion parameters. Thirdly, cables are driven by the motors and Snake Arm gestures are obtained. Image information collected by CCD camera which is settled at the end of the Snake Arm will be displayed on the user interface screen, which makes it obvious to find leakage areas of the fuel tank.

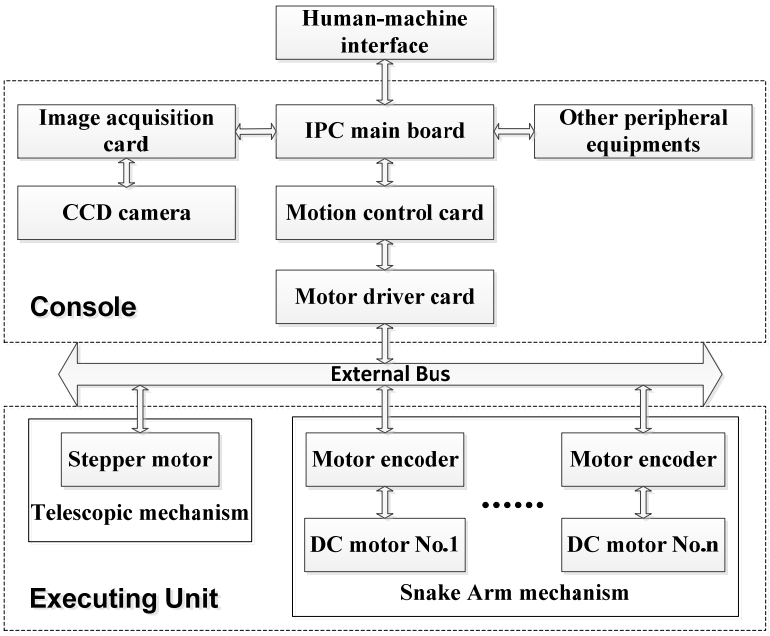

Figure 2. Configuration diagram of control system

2) Console: The subject of the console is actually an industrial personal computer (IPC), including IPC motherboard, supporting parts and peripheral equipments. Motion control card, motor drive card and image acqusition card constitute the supporting parts. CCD camera, external power supplies, along with the input/output devices, such as keyboard and liquid crystal display, consist peripheral equipments. Each motion control card comprises PCI bus interface and four channels which can control two motor driver cards. Each motor driver card is integrated PID and feedforward control algorithm, and can control two motors. Image acqusition card supports VC, VB, Delphi, C++ Builder development.

3) Executing unit: Executing unit comprises the Snake Arm mechanism and the telescopic mechanism. The Snake Arm mechanism has six DC motors with encoders, drives twelve cables and realizes bending and rotation of three section segments in total. A stepper motor and a lead srew make up the telescopic mechanism, realizing the ascent and descent of robot.

3. Kinematics Analysis

This part includes kinematics analysis of single section and multi-section.

3.1. Kinematics Analysis of Single Section

The kinematics analysis of traditional discrete robot is usually based on the Denavit-Hartenberg (D-H) method. Unlike traditional robots composed of joints and rigid links, however, the standard D-H method can't be applied to the kinematics of continuum robots which contain no prismatic or revolute joints. The cable driven robot is different from other robots directly driven by the electric motor. So, kinematics analysis must also take the length variations of driving cables into consideration. In order to get the forward kinematics and inverse kinematics

of single section, the mapping relationship among lengths of cables Δl_i (i =1,2,3,4), two angle variables (bending angle θ and rotation angle ϕ) and tip coordinates (position and orientation of the tip) are established.

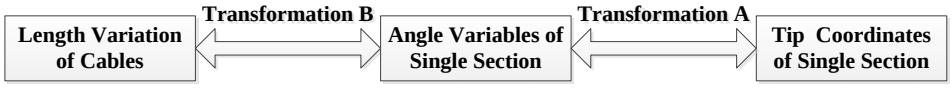

Figure 3. Kinematics model of single section

Figure 3. shows the kinematics analysis of single section, and it includes two transformations: transformation A and B. The former exists between joint space and operation space, and transformation B exists between drive space and joint space.

a) Transformation A

In order to establish relationship between two joint variables (θ and ϕ) and the tip coordinates, a homogeneous transformation matrix (HTM) *T* is established. By analysising transformation from the tip frame to the base frame, T can be expressed by Equation (1).

$$T = Trans(\frac{l}{\theta}\cdot c\phi\cdot(1-c\theta),\frac{l}{\theta}\cdot s\phi\cdot(1-c\theta),\frac{l}{\theta}\cdot s\theta)\cdot Rot(z,\phi)\cdot Rot(y,\theta)\cdot Rot(z,-\phi)$$
$$= \begin{bmatrix} c^2\phi c\theta + s^2\phi & c\phi s\phi c\theta - c\phi s\phi & c\phi s\theta & \frac{l}{\theta}c\phi(1-c\theta) \\ s\phi c\theta c\phi - s\phi c\phi & s^2\phi c\theta + c^2\phi & s\phi s\theta & \frac{l}{\theta}s\phi(1-c\theta) \\ -s\theta c\phi & -s\theta s\phi & c\theta & \frac{l}{\theta}s\theta \\ 0 & 0 & 0 & 1 \end{bmatrix} \quad (1)$$

where, l represents the length of single section, s and c are respectively short for functions of $\sin$ and $\cos$.

Conversely, we can also get the angle variables after we establish the tip frame matrix. It is supposed that $\vec{n}$, $\vec{o}$, $\vec{a}$ separately represent the separate unit vector of tip coordinate and $\vec{p}$ represents the position vector from base frame to tip frame. Then $\vec{n}$, $\vec{o}$, $\vec{a}$, $\vec{p}$ can be expressed as following:

$$T_H = [\vec{n},\vec{o},\vec{a},\vec{p}] = \begin{bmatrix} n_x & o_x & a_x & p_x \\ n_y & o_y & a_y & p_y \\ n_z & o_z & a_z & p_z \\ 0 & 0 & 0 & 1 \end{bmatrix} \quad (2)$$

Given end position and gesture of single section, the two angle variables can be obtained by Equation (3) as following:

$$\begin{cases} \theta = \arccos(a_z) \\ \phi = \arctan\left(\frac{p_y}{p_x}\right) \end{cases} \quad (3)$$

The unique solution of θ is obtained through Equation (3), the interval of the rotation angle ϕ ,is [0,2π],if $p_x \le 0$, The only solution among [π/2,3π/2] of φ can be got; if $p_x > 0$,the other only solution is among [0,π/2) and (3π/2,2π].

b) Transformation B

The bending and rotation of the continuous section rely mainly on the length variation of the four driving cables. In the bending process, bending angle of driving cable equals to that of flexible supporting rod. However, there exists a position offset between driving cable and the supporting rod, and the bending radius of each driving cable is different from that of supporting rod.

When single section bends and rotates, curves of four driving cables are mapping on the bending planar of supporting rod, as is shown in Figure 4.

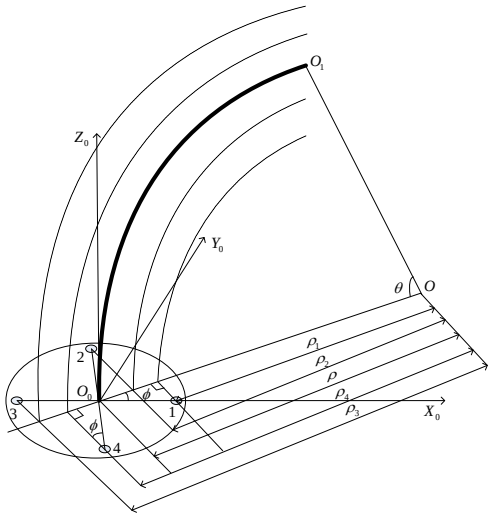

Figure 4. Curved schematic diagram of single section

According geometric relations, the length changes of four driving cables is expressed as:

$$\begin{cases} \Delta l_1 = (\rho - \rho_1)\cdot\theta = r\cdot\theta\cdot\cos\phi \\ \Delta l_2 = (\rho - \rho_2)\cdot\theta = r\cdot\theta\cdot\cos(\phi - \pi/2) \\ \Delta l_3 = (\rho - \rho_3)\cdot\theta = r\cdot\theta\cdot\cos(\phi - \pi) = -\Delta l_1 \\ \Delta l_4 = (\rho - \rho_4)\cdot\theta = r\cdot\theta\cdot\cos(\phi - 3\pi/2) = -\Delta l_2 \end{cases} \quad (4)$$

Where ρ represents the curvature radius of supporting rod, ρ_i(i=1,2,3,4) represents the curvature radius of the i-th driving cable.

From Equation (4), we can conclude that the length change quantity of 1# driving cable opposites that of 3# driving cable, and the length change quantity of 2# driving cable opposites that of 4# driving cable. Therefore, we can twine these two driving cables on the same motor shaft in the opposite direction, then one motor can drive two driving cable, namely, single section can be drived by two motors.

3.2. Kinematics Analysis of Multi-section

The Snake Arm is constructed of connecting many sections in series, and we can solve kinematics function in the way we solve the tandem machine kinematics method. Coupling occures when multiple sections acts collaboratively, and the priority to decouple is to calculate HTM between the sections. Assuming HTM that the section frame {i} relatives to {i-1} is ${}^{i-1}_{i}T$, the HTM of frame {i} relative to frame {j} can be expressed by Equation (5).

$$ {}_{i}^{j}T = {}_{j+1}^{j}T \cdot {}_{j+2}^{j+1}T \cdots {}_{i}^{i-1}T \tag{5} $$

Where, ${}_{i}^{j}T$ is given by Equation (6).

$$ {}_{i}^{i-1}T = \begin{bmatrix} c^2\phi_i c\theta_i & c\phi_i s\phi_i c\theta_i - c\phi_i s\phi_i & c\phi_i s\theta_i & \frac{l}{\theta_i}\cdot c\phi_i \cdot (1-c\theta_i) \\ c\phi_i s\phi_i c\theta_i - c\phi_i s\phi_i & s^2\phi_i c\theta_i + c^2\phi_i & s\phi_i s\theta_i & \frac{l}{\theta_i}\cdot s\phi_i \cdot (1-c\theta_i) \\ -c\phi_i s\theta_i & s\phi_i s\theta_i & c\theta_i & \frac{l}{\theta_i}\cdot s\theta_i \\ 0 & 0 & 0 & 1 \end{bmatrix} \tag{6} $$

Where θ_i and ϕ_i respectively denote the bending angle and rotation angle of i# setion relative to (i-1)# section.

A mapping relationship between the joint variables and endpoint position vector of the multi-section is established.

Snake Arm is composed of several continuous sections, and all drive motors are installed on the base, so driving cables of the the later section pass through the supporting disks' hole of front section. Assuming that the number of sections is N and every hole is threaded a cable at least, thus the total number of holes circling on the supporting disk is n (n=4N). There is a offset angle $\Delta\alpha$ ($\Delta\alpha = (2\pi)/n$) to make driving cables apart from each other. So, the offset angle and the coupling effects of front sections should be taken into consideration to get the decoupling formula between joint variables and lengths of each section's driving cables.

Among the four driving cables of each section, we provide that in this paper, the first driving cable is the one which is between positive directions of X_0-axis and Y_0-axis in the base frame. So in the process of multi-section coupling movement, the length change of i# section's m# ($m = 1, 2, 3, 4$) driving cable is the coupling of total length changes of 1# to i# section. In that way, it can be calculated as Equation (7):

$$ \Delta L_m^i = \sum_{k=1}^{i} \Delta l_{k,(i+N\cdot(m-1))} \tag{7} $$

Where $i = 1, 2, \cdots, N$, $\Delta l_{i,j}$ is the length change of i# section through j# hole, it can be given by Equation (8).

$$ \Delta l_{i,j} = -\Delta l_{i,(j+2N)} = r\cdot\theta_i \cdot \cos(\phi_i - (j-1)\cdot\Delta\alpha), \quad j = 1, 2, \cdots, 2N \tag{8} $$

4. Results and Analysis

In order to validate the adaptability of designed aircraft fuel tank inspection robot, kinematics simulations and prototype experiments are carried out in the following.

4.1. Kinematics Simulation

In the discrete robot moving process, the rigidity of the structure and shape of the traditional robot itself remain unchanged, while continuum robot itself will change its shape, and thus its workspace also changes. The single section's workspace analysis is analysed in this paper. We can get the analysis of single section based on Equation (2), where the length of single section is 25cm, the range of bending angle θ is (0, π] and the range of rotation angle φ is [0, 2π]. According to the following parameters, the workspace of single section is obtained.

Figure 5 shows the workspace of single section which is simulated with Matlab. As is shown in Figure 5, within the range of rotation angle and bending angle, the workspace of the single section forms a spherical cap.

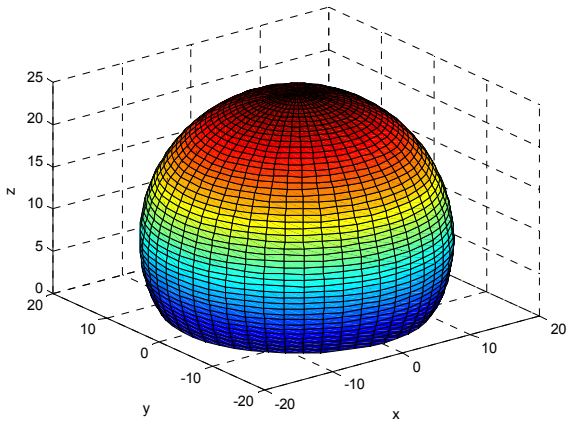

Figure 5. Workspace of single section for continuum robot

In order to study the lengths changes of four driving cables of single section when the robot bends and rotates, Matlab simulations are performed. In initial situation, the rotation ϕ, the bending angle θ and length change of each driving cable are set to be zero (θ is infinitely close to zero but not equals zero), and the end coordinates of the robot is $[0,0,25]^T$. While bending angle θ and rotation ϕ are seperately among (0, π] and [0,2π] and the sampling times is 50, according to Equation (4), we get length changes of four driving cables for the single section as is shown in Figure 6.

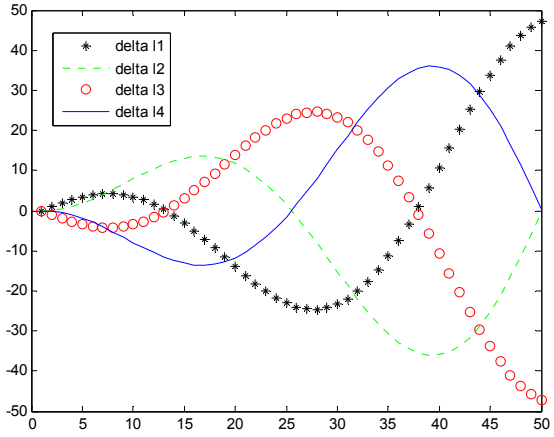

Figure 6. Length changes of cables for single section

4.2. Prototype Experiments

In order to inspect the internal leak of aircraft fuel tank, the snake-like robot needs the ability of flexible bending and rotating in three-dimensional space. A prototype of continuum robot is designed to achieve the inspection task. As shown in Figure 7, three sections driven by 6 DC servo motors can bend and rotate omidirectionally in the space and the prototype robot can bend to form a smooth, complex plannar or spatial curve with high dexterity.

Figure 7. Space motion experiment the robot with three sections

The aircraft fuel tank is full of explosive fuel gas, so any collision and friction are inhibited in the process of inspecting. Therefore a precise kinematic formula must be guaranteed. In order to verify the correctness of kinematics analysis, the verification experiment is established. So maximum deviation equation of the position changes in the experiment is given by Equation (9).

$$\delta_{\max} = \max\left\{\left|x_p - x_t\right|, \left|y_p - y_t\right|, \left|z_p - z_t\right|\right\} \tag{9}$$

Where, $\left(x_p, y_p, z_p\right)$ and $\left(x_t, y_t, z_t\right)$ represent respectively practical and theoretical coordinates of target point.

In order to analysis the deviation between theoretical and practical values in prototype experiments, we choose four postures of the Snake Arm. The bending angle and rotation angle of i# section is respectively θi and φi (i=1,2,3). As is shown in Table 1, the maximum deviation is about 4.34 cm. Considering these datas, we can find that there are some errors in the multi-section movement, and this is mainly because of the accumulation of error of each section, when the robot moves, the stiffness of the glass fiber rod is not great enough. In order to improve the accuracy of the multi-section movements, a better choice of materials is essential. Although there exists errors, they are allowable in practical inspection. All these experiments indicate that the kinematics model proposed is correct.

Table 1. Error Analysis of Four Postures

	θ1,θ2,θ3(°)	φ1,φ2,φ3(°)	theoretical coordinates of target point (cm)	practical coordinates of target point (cm)	δ_{max}(cm)
1	0,0,60	0,0,0	（11.94,0,70.67）	（7.6,0.6,71.1）	4.34
2	0,0,60	0,0,30	（10.34,5.97,70.67）	（11.25,4.07,71.43）	1.90
3	0,30,60	0,90,30	（10.34,21.90,63.79）	（13.82,25.01,62.73）	3.48
4	10,30,60	30,180,90	（-8.45,16.72,67.50）	（-10.15,15.48,65.65）	1.85

5. Conclusion

A novel continuum robot for aircraft fuel tank inspection is developed in this paper. The robot which has a total of six DOF is divided to three sections, and each section is driven remotely by two DC servo motors through cables. Also, the kinematics model of single section is discussed in this paper. Based on the kinematics of single section, the decoupling kinematics of multi-section is deduced. Then, simulation about workspace of single section is presented and the prototype experiments are carried out to verify the kinematics model and show the motion performance. Experiment results indicate the kinematics model is correct. The robotic inspector

is adaptable to complex environment of fuel tank, and its ability of bending and rotation can make the robot itself to achieve a complex planar or spatial curve with high dexterity.

Acknowledgements

This work was funded by the Fundamental Research Funds for the Central Universities #ZXH2011D008. The support by Robotics Institute of Civil Aviation University of China was acknowledged.

References

[1] G Robinson, JBC Davies. *Continuum Robots - A State of the Art*. IEEE International Conference on Robotics and Automation. Detroit, Michigan. 1999: 2849-2854.
[2] Walker ID, Hannan MW. *A Novel 'elephant's trunk' Robot*. IEEE International Conference on Advanced Intelligent Mechatronics. Atlanta. 1999: 410-415.
[3] ID Walker, C Carreras, R McDonnell, G Grimes. Extension versus Bending for Continuum Robots. *International Journal of Advanced Robotic Systems*. 2006; 3(2): 171-178.
[4] BA Jones, ID Walker. *Three-Dimensional Modeling and Display of Continuum Robots*. IEEE International Conference on Intelligent Robots and Systems. Beijing, China. 2006: 5872-5877.
[5] BA Jones, ID Walker. *Limiting-case Analysis of Continuum Trunk Kinematics*. IEEE International Conference on Robotics and Automation. Roma, Italy. 2007: 1363-1368.
[6] Simaan N. *Snake-like Units Using Flexible Backbones and Actuation Redundancy for Enhanced Miniaturization*. IEEE International Conference on Robotics and Automation. Barcelona, Spain. 2005: 3012-3017.
[7] K Xu, N Simaan. *Actuation Compensation for Flexible Surgical Snake-like Robots with Redundant Remot Actuation*. IEEE International Conference on Robotics and Automation. Orlando, Florida. 2006: 4148-4154.
[8] K Xu, N Simaan. An Investigation of the Intrinsic Force Sensing Capabilities of Continuum Robots. *IEEE Transactions on Robotics*. 2008; 24(3): 576-587.
[9] DB Camarillo, CF Milne, CR Carlson, MR Zinn, JK Salisbury. Mechanics Modeling of Tendon-driven Continuum Manipulators. *IEEE Transactions on Robotics*. 2008; 24(6): 1262-1273.
[10] DB Camarillo, CR Carlson, JK Salisbury. Configuration Tracking for Continuum Manipulators with Coupled Tendon Drive. *IEEE Transactions on Robotics*. 2009; 25(4): 798-808.
[11] G Chen, MT Pham, T Redarce. *A Semi-autonomous Micro-robotic System for Colonoscopy*. IEEE International Conference on Robotics and Biomimetics. Bangkok, Thailand. 2009: 703-708.
[12] G Chen, MT Pham, T Redarce. Sensor Based Guidance Control of a Continuum Robot for a Semi Autonomous Colonoscopy. *Robotics and Autonomous Systems*. 2009; 57: 712-722.
[13] RJ Webster, JM Romano, NJ Cowan. *Kinematics and Calibration of Active Cannulas*. IEEE International Conference on Robotics and Automation. Pasadena, CA. 2008: 3888-3895.
[14] RJ Webster, JM Romano, NJ Cowan. Mechanics of Precurved-Tube Continuum Robots. *IEEE Transactions on Robotics*. 2009; 25(1): 67-78.
[15] Hu HY, Li MT, Wang PF, Feng Y, Sun LN. Development of a Continuum Robot for Colonoscopy. *High Technology Letters*. 2009; 15(2): 115-119.